Published in final edited form as:
Dev Biol. 2008 September 15; 321(2): 407–419. doi:10.1016/j.ydbio.2008.07.005.

Growth of cranial synchondroses and sutures requires polycystin-1

Elona Kolpakova-Hart[1], **Brandeis McBratney-Owen**[1], **Bo Hou**[1], **Naomi Fukai**[1], **Claudia Nicolae**[1], **Jing Zhou**[2], and **Bjorn R. Olsen**[1,*]

1*Department of Developmental Biology, Harvard School of Dental Medicine, Boston, Massachusetts 02115, USA*

2*Renal Division, Department of Medicine, Brigham and Women's Hospital and Harvard Medical School, Boston, MA 02115, USA*

Abstract

In vertebrates, coordinated embryonic and postnatal growth of the craniofacial bones and the skull base is essential during the expansion of the rostrum and the brain. Identification of molecules that regulate skull growth is important for understanding the nature of craniofacial defects and for development of non-invasive biologically based diagnostics and therapies.

Here we report on spatially restricted growth defects at the skull base and in craniofacial sutures of mice deficient for *polycystin-1* (*Pkd1*). Mutant animals reveal a premature closure of both presphenoid and sphenooccipital synchondroses at the cranial base. Furthermore, knockout mice lacking *Pkd1* in neural crest cells are characterised by impaired postnatal growth at the osteogenic fronts in craniofacial sutures that are subjected to tensile forces. Our data suggest that polycystin-1 is required for proliferation of subpopulations of cranial osteochondroprogenitor cells of both mesodermal and neural crest origin during skull growth. However, the Erk1/2 signalling pathway is up-regulated in the *Pkd1*-deficient skeletal tissue, similarly to that previously reported for polycystic kidney.

Keywords

Craniofacial skeleton; Craniosynostosis; Cranial base; Synchondrosis; Suture; Polycystin-1

Introduction

Craniosynostosis or premature suture fusion is a wide spread disorder occurring in 300-500 out of 1,000,000 live births. In humans, premature closure of cranial base synchondroses or sutures followed by reduced growth of the skull along the rostral-caudal axes have been implicated in both syndromic and single suture craniosynostoses. Presence of multiple cases within a family and prevalence of craniofacial defects involving skull base growth in certain ethnic groups strongly suggest a contribution of a genetic component to determination of craniofacial morphology (Singh, 1999). Thus, identification of candidate genes that regulate

* Author for correspondence (e-mail: bjorn_olsen@hms.harvard.edu), Address: Department of Developmental Biology, Harvard School of Dental Medicine, Boston, Massachusetts 02115, USA, Telephone: +1-617-432-1874, Fax: +1-617-432-0638.

development and postnatal growth of the craniofacial skeleton is important for further understanding of the mechanism underlying skull abnormalities. Moreover, characterization of molecular pathways involved in suture growth would facilitate the design of biologically based treatments, which can substitute or complement currently available surgical procedures. In the present study, we have studied mechanisms of craniofacial bone and skull base growth in conditional knockout mouse strains of polycystin-1 (*Pkd-1*).

The gene encoding polycystin-1, *PKD1*, was first identified by positional cloning as a gene mutated in 85% of patients with autosomal dominant polycystic kidney disease (ADPKD) and its role in renal pathology and kidney development has been intensively studied (The European Polycystic Kidney Disease Consortium, 1994). Polycystin-1 is an integral membrane glycoprotein with a large extracellular domain, proposed to mediate intercellular and cell-matrix interactions. The small intracellular domain has been implicated in signal transduction by activating downstream cytoplasmic effectors (Delmas, 2005). Together with another membrane-associated protein, the non-selective cation channel polycystin-2, polycystin-1 mediates mechanosensory signal transduction in renal epithelial cells (Nauli et al., 2003). In mice, *Pkd1* is broadly expressed in non-renal tissues (Guillaume et al., 1999) and multiple developmental defects, including skeletal and vascular abnormalities, were reported in *Pkd1*-deficient animals. However, the early onset of cyst formation in several internal organs and severe systemic edema resulting in embryonic death obscured the interpretation of other phenotypic anomalies and prevented the analysis of postnatal skeletal functions of polycystin-1 (Boulter et al., 2001;Kim et al., 2000;Lu et al., 2001;Lu et al., 1997).

In this study, we used *Wnt1*-, *Dermo1*- and *Osx1-Cre* to conditionally remove polycystin-1 from most skeletal tissues in mice. The data demonstrate that polycystin-1 is a positive regulator of skeletal mesenchymal cell proliferation in cranial growth regions. Thus, *Pkd-1* deficiency leads to premature closure of the synchondroses at the skull base and impaired postnatal growth of dermal craniofacial bones.

Materials and methods

Mouse strains

Mice harbouring floxed alleles *of Pkd1* were described previously (Starremans et al., 2008). *Dermo1*-Cre, *Wnt1*-Cre and *Osx*-Cre deleter strains were kindly provided by Drs. David Ornitz and Andy McMahon. The presence or absence of the Cre transgenes was determined using PCR with primers specific to the Cre recombinase coding sequence: Cre5′ (TGC TCT GTC CGT TTG CCG) and Cre3′ (ACT GTG TCC AGA CCA GGC).

Skeletal staining and paraffin section preparations

Skin, muscles and visceral organs were removed from embryos or newborn animals prior to overnight incubation in solution containing 0.06% Alizarin red S and 0.02% Alcian blue (Sigma, St. Louis, MO) in a 1:4 mixture of glacial acetic acid and 95% ethanol. Skeletal samples were then cleared by incubation in 1.8% and 0.3% potassium hydroxide and stored in 100% glycerol. The skeletal preparations were analysed and photographed in glycerol/ethanol solution. For histological analysis and in situ hybridisation on paraffin sections, skull preparations were fixed overnight in 4% paraformaldehyde in PBS, dehydrated in ethanol and embedded in paraffin. Paraffin blocks were sectioned at 6μm, sections mounted onto glass slides, de-waxed and processed for hematoxylin and eosin staining or in situ hybridization.

Frozen section preparation and β-galactosidase staining

Skulls of 4-day old pups were dissected and fixed on ice in 4% paraformaldehyde in PBS for 30 min, incubated overnight with 20% sucrose in PBS and embedded in Tissue-Tek OCT

compound (Sakura Finetek USA, Inc., Torrance, CA) with a slurry of solid CO_2 in 95% ethanol. Frozen blocks were sectioned 7μm thick using Leica crytome and air-dried for 30 min. After two washes in 10mM $MgCl_2$ in PBS, samples were treated in detergent for 10 min on ice and stained in solution containing 5mM $K_3Fe(CN)_6$, 5mM $K_4Fe(CN)_6 \cdot 3H_2O$, 1mM $MgCl_2$, 0.01% sodium deoxycholate, 0.009% NP40, 1mg/ml X-gal for 45 min to 3 hours at 37°C. Colour reaction was stopped by postfixation in 4% paraformaldehyde in PBS for 30 min at RT.

In vivo labelling of bone tissue

Calcein (6mg/kg body weight) and alizarin complexon (60 mg/kg body weight) were administered intraperitoneally postnatal day 4 and 2 hours prior to sacrifice on postnatal day 14, respectively. Crania were harvested for analysis, fixed with 4% paraformaldehyde for 2 hours at RT and dehydrated in a series of graded alcohols. Individual cranial bones were dissected out and mounted on slides using EUKITT mounting medium (Electron Microscopy Sciences, Hatfield, PA). The sections were examined using a conventional (80i Upright Microscope, Nikon, Japan) or confocal (C1, Nikon, Japan) fluorescence microscopes. Images were obtained and analysed using Metamorph 7.0 and EZ-C1 software.

BrdU, phospho-histone 3, TUNEL staining and in situ hybridisation

BrdU (Sigma, St. Louis, USA) was injected intraperitoneally at concentration 50μg/g body weight 2 hours before sacrifice. Skeletal tissue of interest was harvested, fixed overnight at 4° C in 4% paraformaldehyde and decalcified in 0.5M EDTA for 2 weeks. Decalcified samples were embedded in paraffin and sectioned 6 μm thick. BrdU-positive cells were detected using BrdU staining kits (Zymed Laboratories Inc., San Francisco, CA). Apoptotic cells were visualized using DeadEnd™ Fluorometric TUNEL system (Promega Corporation, Madison, WI). Phosphorylated histone H3-specific antibody were purchased from Cell Signalling Technology (Beverly, MA) and used for immunocytochemical experiments in accordance with the manufacturer's recommendations. In situ hybridisation was performed as described previously (Kolpakova-Hart et al., 2007).

Western blotting

Frontonasal suture and osteogenic front tissue was dissected and cells separated from the extracellular matrix during a 4 hr incubation with collagenase P (1mg/ml, Roche), and 0.01% trypsin at 37 °C. Cell suspension was put through a 70μm cell strainer (BD Falcon) and lysed in ice-cold RIPA buffer (50mM Tris pH 7.5, 150mM NaCl, 2mMEDTA, 1% NP-40, 0.5% Na-deoxycholate, 0.1% SDS) supplemented with proteinase inhibitors. Aliquots of cell lysates (60μg) were separated on 10% sodium dodecyl sulfate-polyacrylamide gels and transferred to nitrocellulose membranes. The membranes were blocked with 5% dry fat-free milk in PBS for 1 hour and incubated overnight at 4°C with primary antibody in Tris-buffered saline (TBS) and 0.1% Tween 20. Membranes were washed and incubated with secondary antibody conjugated to horseradish peroxidase (Pierce,1:5000). Signal detection was performed using the Super Signal West Femto Maximum Sensitivity Substrate (Pierce, Rockford, IL). The p-p38 MAPK (#9211) and p-Erk1/2 (#4376) antibodies were from Cell Signaling and used at dilution 1:1000. p21-specific antibody were obtained from Santa Cruz (1:500; C19, sc-397).

Results

Genetic inactivation of Pkd1 results in delayed ossification, malocclusion, skull base synostosis and retarded postnatal growth of the craniofacial complex

Cranial neural crest cells (NCC) contribute extensively to the neck and anterior skeleton of the head, whereas the skeletal elements in the posterior skull, trunk and limbs are derived from somitic and lateral plate mesoderm. NCC-specific gene targeting using *Wnt1*-driven Cre

recombinase (Brault et al., 2001) has been employed in several studies of craniofacial development (Brewer et al., 2004;Dudas et al., 2004). To investigate a role of polycystin-1 in the cranial neural crest mesenchyme, we performed *Pkd1* inactivation by crossing the *Wnt1*-Cre transgenic animals with *Pkd1* floxed mice. Conditional *Wnt1-Cre; Pkd1* knockout mutants were born in Mendelian ratio and appeared normal. However, a delay in intramembranous ossification of the skull was observed (Fig.S1A). Three weeks after birth, mutant animals could be distinguished from their control littermates by a shortened snout and a dome-shaped skull vault (Figs. 1A and 1B). In addition, the growth of the upper jaw was profoundly retarded leading to an abnormal apposition of the incisors (class III malocclusion) (Fig. 1B). Preparations of the individual cranial bones from adult mutant mice revealed that the frontal bones and mandible were only slightly affected, whereas the nasal, pre-maxillary and maxillary bones were severely reduced in length (Fig. 1C). Analysis of the cranial base revealed that the most anterior synchondrosis (presphenoid, PSS) was obliterated in the mutant animals, leading to shortening of the sphenoid and presphenoid bones (Fig. 1D). The sphenooccipital synchondrosis (SOS) remained patent in both mutants and their wild-type littermates.

To visualize neural crest-derived skeletal tissue in the postnatal skull, we crossed *Wnt1*-Cre mice with the conditional *LacZ* reporter mouse strain *Rosa 26R*, in which β-galactosidase expression is activated by Cre recombinase (Soriano, 1999). Analysis of the skull of the *Wnt1-Cre;R26R* animals at postnatal day 4 suggested that contribution of the neural crest cell population to the cranial base was restricted to its anterior part, as only the presphenoid and sphenoid bones were *Wnt1-Cre* positive. The anterior cranial base suture, the presphenoid synchondrosis, consisted entirely of β-galactosidase-positive cells, whereas no activity of the enzyme was detected within the posterior sphenooccipital synchondrosis (Fig. S1B).

We next investigated the potential role of polycystin-1 in a broad range of osteochondroprogenitor cells in the cranial, axial and appendicular skeleton using Cre recombinase regulated by the promoter of the mesoderm-specific basic helix-loop-helix transcription factor *Dermo1* (Yu et al., 2003). *Dermo1-Cre* deleter mice have been previously characterized (Yu et al., 2003) and successfully used for gene targeting in skeletal tissues (Day et al., 2005;Kolpakova-Hart et al., 2007;Yu et al., 2003). At birth, the *Dermo1-Cre; Pkd1* animals displayed a delay in ossification of the cranial, axial and appendicular skeleton (data not shown). In addition, mutant pups often displayed slow growth and reduced body weight. A close examination of conditional knockout animals revealed development of multiple cysts in the kidney (Fig. S2A). During development, kidneys originate from the intermediate mesoderm, localized between the somites and the lateral plate (Saxen and Sariola, 1987). Using the Rosa reporter strain, we confirmed that *Dermo1-Cre* is expressed in the mesoderm-derived kidney epithelium and interstitial mesoderm (Fig. S2B). Therefore, the polycystic kidney phenotype observed in the *Dermo1-Cre;Pkd1* mice was due to kidney-specific *Pkd1* inactivation. However, all *Dermo1-Cre;Pkd1* mutants displayed a characteristic dome-shaped skull, indicating defects in the postnatal growth of the cranial bones (Fig. 2A). Upon close examination of the mutant skull base, we observed an ossified bridge within the central area of the SOS (Fig. 2B). In order to understand the origin of this postnatal growth defect, we compared the developmental changes within the prospective SOS in the control and mutant embryos.

During embryogenesis, the presumptive SOS is formed after the pituitary gland becomes separated from the roof of the mouth. In the cranial base, it is located between two patches of undifferentiated mesenchyme: hypophyseal and basicranial fenestrae, which are normally present in the early embryonic chondrocranium, but disappear as they become populated with skeletogenic tissue before birth. In the *Pkd1*-deficient skulls, the cranial base fenestrae were found abnormally enlarged (Fig. 2C) and persisted during late embryogenesis and after birth. In vivo double labelling of bone tissue with calcein/alizarin demonstrated that ectopic

ossification of SOS in *Dermo1-Cre; Pkd1* mice impairs the postnatal longitudinal growth of the cranial base (Fig. 2D). Closure across SOS was progressive with age and a complete fusion was observed in all adult mutant mice (Fig. 2E). Similar to *Wnt1-Cre;Pkd1* conditional knockout mice, premature closure of the presphenoid synchondrosis within the first postnatal week was observed in *Dermo1-Cre; Pkd1* mutant pups (Fig. S2C, left panel). Thus, unlike *Wnt1-Cre;Pkd1* mutants in which only PSS underwent premature closure, both PSS and SOS were affected in the cranial base of the *Dermo1-Cre;Pkd1* animals. That is in agreement with the observation that *Dermo1-Cre* is expressed in both synchondroses and is not restricted to neural crest mesenchyme (Fig. S2C, right panel).

Pkd1-deficient synchondrosal chondrocytes and chondroprogenitor cells exhibit reduced proliferative activity

Normal embryonic and postnatal growth of the skull base largely depends on a fine balance between proliferation and differentiation of chondrocytes in the cranial base sutures (i.e; synchondroses). Upon visual inspection, no morphological difference was observed between newborn *Wnt1-Cre;Pkd1* mutants and control littermates. By day four after birth, the first changes in the mutant anterior cranial base were detected and manifested in diminished size of the presphenoid synchondrosis (Fig. 3A). Within the next two days, the synchondrosal area occupied by proliferating and resting chondrocytes was limited to a small circular patch of cells surrounded by hypertrophic chondrocytes. Eventually, remnants of the growth plate were displaced dorsally and the synchondrosis was substituted by bone (Fig. 3B).

The cranial base growth deficiency in the absence of *Pkd1* could be caused by abnormal differentiation of synchondrosal growth plates, decreased survival and/or proliferation of chondrocytes. To test these possibilities, we analysed the distribution of collagen X, a specific extracellular matrix protein produced by chondrocytes as they differentiate and become hypertrophic. The expression of this marker was restricted to the periphery of the mutant and control synchondroses, the typical location for hypertrophic chondrocytes within a growth plate (Fig. 3C). Spatial distribution and expression levels of type II collagen, osteopontin, type I collagen and Indian hedgehog were not changed (Figs. 3D, 3E and data not shown).

To examine chondrocytic proliferative activity, we performed in vivo BrdU labelling and immunostaining on paraffin sections. The number of dividing cells in the proliferative zone of the mutant PSS was markedly decreased (Fig. 4A). We did not observe differences in BrdU labelling between the mutant and control SOS (data not shown). These results suggested that proliferative activity of chondrocytes within the pre-sphenoid synchondrosis was altered, causing the premature closure of PSS and limited postnatal growth of the basisphenoid and presphenoid bones. Similar observations were made during the PSS closure of in *Dermo1-Cre;Pkd1* mice (data not shown).

To assess cell viability, we also performed TUNEL staining of the affected synchondrosis prior to its fusion. We did not detect any apoptosis in the mutant or control chondrocytes. However, we observed a population of apoptotic cells in the perichondrium of the mutant PSS prior to its closure, suggesting that polycystin-1 might be essential for survival of perichondrial cells (Figs. 4B and 4C).

In order to understand the developmental defects that cause the postnatal ossification of the sphenooccipital synchondrosis in *Dermo1-Cre* mice, we further examined skeletal preparations and histology of the skull base in E12.5 –E15.5 embryos. Invariably, the cellularity and the overall thickness of the skull base were reduced in the *Pkd1* mutants at all embryonic stages (Fig. 5A). At E13.5 control embryos, the skull base area underlying the newly formed pituitary gland was already occupied by fully differentiated chondrocytes, whereas the corresponding region in the mutants, was populated by undifferentiated mesenchymal cells (Figs. 5A and 5B).

In addition to delayed differentiation, the mesenchymal cells that occupied the presumptive SOS area displayed decreased proliferative activity, as measured by BrdU incorporation (Figs. 5B and 5C).

Interstitial and endochondral growth of the nasal septum is normal in Wnt1-Cre;Pkd1 mice

To understand the nature of the growth defect of the upper jaw observed in *Wnt1-Cre; Pkd1* mice, we first compared the postnatal growth of the cartilaginous nasal septum and the ethmoid bone, which support the craniofacial skeleton in the mid-line. Levels of interstitial chondrocytic proliferation in the nasal septum were evaluated using immunohistochemical labelling of phosphorylated histone 3 and BrdU incorporation. No significant differences were detected between the *Pkd1*-deficient and control nasal cartilages at postnatal day 2, when the interstitial proliferation normally occurs (Fig. 6A). Moreover, we did not observe cell death or evidence of decreased secretion of the extracellular matrix by chondrocytes later during the elongation of the nasal cartilage (data not shown).

We next examined whether endochondral growth of the ethmoid bone, which is continuous with the caudal nasal septum and contributes to the anterior-posterior elongation of the upper jaw, is affected by polycystin-1 inactivation. Differential in vivo double labelling of the newly formed bone, did not reveal any difference in the growth rate of mutant and control ethmoid bones between postnatal day 4 and 14 (Fig. 6B). During the first 2 weeks after birth, the mutant nasal cartilage continued to increase in length, but its advancement in the rostral direction was impaired due to the lack of nasal bone growth. This led to a characteristic bent morphology of the nasal septum and its displacement from the mid-line in all knockout pups (Fig. 6C). These data indicate that the morphological changes detected in nasal cartilage by the second postnatal week are secondary to the facial bone growth defect.

Postnatal growth of the posterior nasal and premaxillary bones is impaired due to reduced proliferation of the sutural osteoprogenitor cells

Using the method of in vivo double labelling of bone tissue with calcein and alizarin, we evaluated the postnatal growth of the nasal bone during the first two weeks after birth. At postnatal day 4, the mutant and control nasal bones were comparable in shape and size, albeit a markedly reduced bone matrix deposition was evident in the mutant dermal bones at that stage (Fig. 6D, middle panel). Ten days later, mineralization occurred in both rostral and caudal directions in the control nasal bone (Fig. 6D, top left and right panels). Growth of the rostral nasal bone proceeded normally in mutant mice as well, whereas the elongation of its caudal part was significantly reduced (Fig. 6D, bottom left and right panels). The growth of the premaxillary bone was also affected but to a lesser degree.

Sutures of dermal bones are composed of mesenchymal cells and serve as growth sites of the cranium. In order to understand the nature of the growth defect observed in the *Pkd1*-deficient facial bones, we examined histological sections of the early postnatal frontonasal (FN) and frontopremaxillary (FP) sutures. Despite differences in the overall morphology between the frontonasal and frontopremaxillary sutures, they both appeared as bands of mesenchymal cells, which separate the osteogenic fronts of the adjacent bones. Histological studies revealed no premature suture closure, as both FN and FP sutures remained patent in control and mutant animals (data not shown). To evaluate proliferative activity of the sutural osteoprogenitor cells, BrdU labelling of the mesenchymal cells was performed. In control mice, most BrdU-positive cells were detected within the osteogenic fronts of the nasal and premaxillary bones (Fig. 7A, upper panel). Fewer dividing cells were found in locations adjacent to the surface of the frontal bone. Such asymmetric distribution of proliferating cells can be due to the fact that the frontal bone grows at a slower rate in comparison to the nasal and premaxillary bones. A limited number of proliferating cells was detected in the mutant frontonasal suture, whereas the

population of BrdU-positive cells in the frontopremaxillary suture was significantly reduced (Figs. 7A, and 7B).

Conceivably, the growth abnormalities observed in the *Pkd1*–deficient cranial sutures could be due to proliferation or differentiation defects in osteoblastic cells rather than in mesenchymal osteoprogenitor cells. In order to test this possibility, we inactivated *Pkd1* in early osteoblastic cells using Cre recombinase driven by *Osterix*-specific promoter (Rodda and McMahon, 2006). The *Osx-Cre;Pkd1* conditional knockout mice displayed a delay in intramembranous ossification, but no growth defects of the craniofacial bones. The length of the mutant nasal and premaxillary bones was comparable to control bones, suggesting that the craniofacial bone growth deficiency observed in *Pkd-1* mutants was not due to defective osteoblasts (Fig. S3 and data not shown).

Up-regulation of Erk1 and Erk2 activity in Pkd1-defficient osteoprogenitor cells

We have also attempted to gain insight into the mechanism by which polycystin-1 may control proliferation of osteochondroprogenitor cells. We have dissected frontonasal and fronto-premaxillary suture cells from *Wnt1*-Cre; *Pkd1* mutant mice and their normal littermates at P10-P12 and performed Western blot analyses with antibodies against phospho-p38 MAPK, Erk1/2, phospho-Erk1/2, Akt, phospho-Akt and cell-cycle inhibitor p21 (Figure 7C and data not shown). We found no difference in p21 protein levels between osteoprogenitor cells from wild-type and *Pkd1*-deficient mice. Comparable amounts of Akt were present in both control and *Wnt1*-Cre; *Pkd1* animals, whereas the phosphorylated form of Akt was undetectable (data not shown). Phosphorylation of p38 MAPK was not affected by *Pkd-1* inactivation. In contrast, *Pkd1*-deficiency in suture cells resulted in significantly increased levels of phosphorylated Erk1/2 (Fig. 7C).

Directional orientation of collagen fibres in frontonasal vs. frontopremaxillary sutures is spatially related to the proliferation of osteoprogenitor cells

Different craniofacial sutures in mice display distinct morphology. The frontonasal suture is straight, as opposed to the highly interdigitated, zig-zag-shaped frontopremaxillary suture. Previous studies in several mammalian species suggest that the morphology of the cranial sutures correlates with the polarity and magnitude of the mechanical forces acting on cells within a suture. It has been predicted that blunt-ended sutures result from tension, whereas interdigitated sutures are associated with compressive forces. Accordingly, two different types of collagen fiber arrangement have been suggested: straight orientation of fibers for tensed sutures and oblique orientation for compressed sutures (Rafferty and Herring, 1999). Using confocal fluorescence microscopy we analyzed the organization of the collagen fibers in the FN and FP sutures. We found that the fiber pattern to be consistent with the prediction for both sutures. The FN displayed morphology of a tensed suture with straight collagen fibers stretching across the sutural tissue (Fig. 8A, left panel). In contrast, the FP suture appeared to be a largely compressed suture with obliquely arranged collagen fibers, which provide the best mechanism to resist compression (Fig. 8A, right panel). Interestingly, even within the highly compressed FP suture, there were sites with collagen fibers organized in a manner consistent with the presence of tensile forces. These sites coincided with the locations of active proliferation and directional bone deposition (Fig. 8B). In the frontonasal suture from the wild type mice, proliferating cells were concentrated around the osteogenic fronts of the fast-growing nasal bone (Fig. 8C, left panel). The osteogenic fronts of the growth-retarded *Pkd1*-deficient frontonasal suture appeared blunt-ended with few BrdU-positive cells present (Fig. 8C, right panel).

Discussion

Coordinated growth of cranial bones is essential for accommodating the embryonic and postnatal expansion of the brain. Traditionally, calvarial sutures have been considered as major growth sites of the mammalian skull (Ogle et al., 2004;Opperman, 2000). However, the cranial base, occupying the ventral part of the skull and serving as a supportive platform for the mid-facial skeletal structures, also contributes to the growth of the head skeleton. Furthermore, a coordinated growth of craniofacial bones is important for establishing the proportional spatial relationship between the lower and upper jaws and leads to malocclusion when disturbed.

Multiple synchondroses, which separate bones of the skull base, serve as growth sites during base expansion. Morphologically, a synchondrosis appears as two opposing cartilage growth plates. Analogous to endochondral growth plates in long bones, synchondroses of the skull base grow through a combination of chondrocyte proliferation and hypertrophy. In mice, both the presphenoid and sphenooccipital synchondroses remain patent even in adults. Similar to the epiphyseal growth plate in the long bones, adequate proliferation, differentiation and maturation rates of chondrocytes within the synchondroses are required for longitudinal growth of the cranial base. Previous knockout studies in mice implicate several genes in regulating the postnatal growth of the cranial base. Thus, genetic ablation of the latent TGF-β binding protein (*Ltbp-3*), an extracellular matrix molecule that regulates the bioavailability of TGF-β, results in obliteration of the cranial base synchondroses, a dome-shaped skull and malocclusion (Dabovic et al., 2002b;Dabovic et al., 2002a). However, the mechanism by which Ltbp-3 controls postnatal growth of the synchondroses must be distinct from that of polycystin-1 as premature hypertrophy rather than reduced proliferation of chondrocytes was reported in *Ltbp-3* knockout mice. Inactivation of *Fgfr2* also leads to obliteration of the cranial base synchondroses, overgrowth of low incisors and a dome-shaped skull phenotype (Eswarakumar et al., 2002). However, the mechanism of the impaired synchondrosal growth in the *Fgfr2*-deficient mice was not characterized in detail.

Our data demonstrate that skeletal tissue-specific *Pkd1*-deficiency results in embryonic defects in the mesodermal spheno-occipital synchondrosis and/or postnatal abnormalities in the neural crest-derived presphenoid synchondrosis. In *Wnt1-Cre;Pkd1* mice, only the anterior cranial base synchondrosis (PSS) underwent premature closure, whereas the posterior suture (SOS) remained intact even in adult animals. This is consistent with PSS being of neural crest origin. In contrast, *Dermo1-Cre,* that drives *Pkd1* inactivation in the entire cranial base, causes synchondrosal defects in both PSS and SOS.

Prior to premature postnatal closure of the PSS, we did not detect an early onset of hypertrophy in the mutant synchondroses, and the distribution of the hypertrophic chondrocytes was normal (restricted to the periphery of the growth plates). In contrast, we demonstrated a decreased proliferation of chondrocytes. Although the growth deficiency in the cranial base synchondrosis appears as a cell-autonomous chondrocytic defect, we cannot exclude the possibility that these abnormalities are a result of an indirect effect of the *Pkd1*-deficient perichondrium/periosteum where emergence of apoptotic cells coincides with a decrease in chondrocytic proliferation.

Unlike the postnatal onset of the growth defect within the PSS, abnormalities observed in the SOS of *Dermo-Cre1;Pkd1* conditional knockout mice are due to a specific embryonic defect spatially restricted to the border between the neural crest and the paraxial mesoderm. The presumptive SOS is formed in the location where the oral ectoderm invaginates to form adenopituitary gland and is initially composed of mesodermal chondroprogenitor cells. Between E12 and E13.5, these cells proliferate and differentiate into chondrocytes, as the prospective pituitary gland becomes separated from the roof of the oral cavity. The *Pkd1*-

deficient embryos exhibited a significant decrease in proliferation of mesenchymal osteochondroprogenitor cells in the cranial base. For the mutant prospective SOS, the proliferation level was estimated to be 5-fold lower relative to control. We also observed impaired differentiation of the mesenchymal cells into chondrocytes in the SOS region, which might contribute to the persistence and ossification of the fenestra after birth. Despite the differences in the tissue origin and nature of the defects, both PSS and SOS abnormalities in *Pkd1*-deficient mice lead to reduced postnatal longitudinal growth of the cranial base.

Our data address the important question of what skeletal structure is the primary growth centre of the anterior craniofacial complex. Recently, it has been documented that shortly after birth the cartilaginous nasal septum undergoes active interstitial proliferation followed by rapid expansion in the rostral-caudal direction (Wealthall and Herring, 2006). Normally, during the first two postnatal weeks, both the nasal septum and the nasal bone grow at a high and similar rate. However, it remains unclear whether the expanding nasal septum drives the growth of the surrounding nasal and premaxillary bones. Alternatively, the nasal cartilage may only serve as mechanical support for the craniofacial bones and passively follow their growth in the antero-posterior direction. Because inactivation of *Pkd1* in neural crest cells does not affect proliferation of chondrocytes in nasal cartilage, but does reduce the sutural growth of dermal bones, the postnatal autonomous expansion of the nasal cartilage, which occurs in *Wnt1-Cre;Pkd1* mutant mice, even in the absence of nasal bone growth, strongly suggests an intrinsic ability of the nasal septum to actively contribute to midfacial translation.

The nasal bone is exceptional in its high growth rate. The arrangement of the collagen fibers clearly demonstrates that the frontonasal suture is subjected to tensile forces during growth of the nasal complex. The premaxillary bone is likely to be affected by multiple forces of opposite polarity. The fact that the incisors are located within the premaxillary bone has an impact on the mechanical loading this bone is subjected to. The direct incisal bite applies a compressive force on both premaxilla-maxillary and fronto-premaxillary sutures. The interdigitated nature of fronto-premaxillary suture and the oblique orientation of the collagen fibers along its almost entire surface reflect the presence of compressive loading. On the other hand, the mechanical stress generated by eruption of incisors and by the growth of the nasal septum is likely to exert tensile forces on the premaxillary bone. Accordingly, straight collagen fibers are present along the actively growing tips of the bone.

Based on the analysis of the skull phenotype observed in *Pkd1*-deficient mice we hypothesize that tensile forces within the expanding viscerocranium are necessary for the directional growth of dermal bones and that polycystin-1 is an essential mediator of this process, as it controls proliferation of the mesenchymal cells at the osteogenic fronts. Using *Wnt1-Cre;Pkd1* conditional knockout mice and the technique of mid-palatal suture expansion (Hou et al., 2007), we have tested this hypothesis. The results (Hou B. in preparation) demonstrate that the *Wnt1-Cre;Pkd1* mice display an impaired response to tensile forces in vivo. In this system, induced midpalatal suture expansion in wild type mice triggers proliferation, osteoblastic differentiation of the osteoprogenitor cells within the suture and new bone deposition. In contrast, *Pkd1*-deficient mice exhibit delayed and severely reduced proliferation and differentiation responses of osteoblastic progenitor cells.

Recent in vitro studies have provided evidence that proliferation and differentiation of chondrocytes and osteoprogenitor cells are modulated by mechanical stress (Fitzgerald et al., 2006;Grodzinsky et al., 2000;Kanno et al., 2007;Riddle et al., 2006). In rabbits, tensile forces applied across the frontonasal suture by using an expandable device results in lengthening of the craniofacial complex (Movassaghi et al., 1995). Furthermore, in vivo cyclic and static loading of the cranial base of growing rabbits, induced increased proliferation of chondrocytes leading to an enlargement of the proliferative zone of the cranial base synchondroses (Wang

and Mao, 2002). However, the molecular mechanism underlying the response of suture cells to mechanical strain remains poorly understood. Our data indicate that polycystin-1 is be involved in the process of mechanotransduction and/or response during skull growth. The initial studies of the extracellular domains found in polycystin-1 suggested that this protein can mediate cell-cell and/or cell-extracellular matrix interactions (Hughes et al., 1995). Forman et al. (Forman et al., 2005) used atomic force microscopy to investigate the mechanical properties of the extracellular PKD domains of polycystin-1 and showed that these domains exhibited a remarkable mechanical strength. Based on the structural similarities between polycystin-1 and other modular proteins that have elastic properties, it has been proposed that the protein functions mechanically by providing a flexible and elastic linkage between cells (Qian et al., 2005). Malhas et al., (Malhas et al., 2002) suggested that the leucine-rich repeats (LRR) of polycystin-1 modulated the binding of the protein to various ECM components, such as type I collagen, fibronectin and laminin. Interestingly, addition of the LRR fusion protein to cells grown in culture resulted in a significant dose-dependant reduction in the rate of proliferation. Based on such findings and the experimental data presented in this study, we propose a mechanism by which polycystin-1 might regulate dermal bone growth. According to our model, polycystin-1 displayed on the surface of sutural osteoprogenitor cells interacts with collagen fibers, which relay tensile forces present within a suture. Osteoprogenitor cells, in turn, respond by proliferation, osteoblastic differentiation and directional bone deposition (Fig. 8D).

The mechanism by which polycystin-1 regulates proliferation in chondrocytes and osteoprogenitor cells remains to be elucidated. Previous studies reported that Pkd1 may control cell proliferation through AP-1 or STAT6 -mediated pathways (Arnould et al., 1998;Low et al., 2006;Parnell et al., 2002). It has also been suggested that polycystin-1 and polycystin-2 regulate cell cycle by activating transcription factor Id2 (Li et al., 2005). *Pkd1*-deficiency in kidney resulted in increased proliferation and de-differentiation of tubular epithelial cells. However, our data suggest that inactivation of polycystin-1 in osteochondroprogenitor cells results in reduced proliferation. In contrast to the reduced levels of p21 in kidney epithelial cells lacking *Pkd-1* (Bhunia et al., 2002), we could not detect any difference in the expression of this cell-cycle regulator. Phosphorylation of p38 MAPK was not affected by *Pkd-1* inactivation. In contrast, *Pkd1*-deficiency in suture cells resulted in significantly increased levels of phosphorylated Erk1/2. This is similar to what was reported for polycystic kidney cells in rats and mice (Nagao et al., 2003;Shibazaki et al., 2008). Thus, in both osteoprogenitor and renal cells the presence of Pkd-1 is associated with reduced Erk1/2 phosphorylation; yet, the effects on proliferation are completely different. In the craniofacial sutures, the presence of polycystin-1 is associated with high proliferative activity; in the kidney, the presence of the protein is, apparently, associated with low proliferative activity. Differential cell-type dependent responses to extracellular stimuli have been previously described for a variety of signalling pathways. The outcome seems to largely depend on the repertoire of downstream effectors available in a given cell type. In agreement with this, it has been shown that deficiency in polycystin-2, which is believed to function together with polycystin-1, leads to reduced cell proliferation of lymphoblastoid cells (Aguiari et al., 2004). However, it has also been argued that Erk1/2 activation may not be the underlying basis for increased proliferation observed in cyst-lining cells (Shibazaki et al., 2008).

Recently, hyperactivation of Erk1/2 signalling pathway was linked to premature closure of the coronal suture and cranial base growth defects, caused by constitutively active Fgfr2 (Yin et al., 2008). Moreover, inhibition of Erk1/2 signalling in vivo was reported to prevent craniosynostosis induced by a similar activating mutation in *Fgfr2* (Shukla et al., 2007).

Supplementary Material

Refer to Web version on PubMed Central for supplementary material.

Acknowledgements

We would like to thank Dr. Jennifer Waters and Lara Petrak at the Nikon Imaging Center at Harvard Medical School for professional advice and assistance with microscopy. We thank Sofiya Plotkina for technical assistance and Michael Hart for help with the manuscript. This work was supported by grants R01 AR036819 and R21 AR053143 (to B.R.O.) from the National Institutes of Health. E.K.H was supported by postdoctoral fellowship from the Norwegian Research Council.

References

Aguiari G, Banzi M, Gessi S, Cai Y, Zeggio E, Manzati E, Piva R, Lambertini E, Ferrari L, Peters DJ, Lanza F, Harris PC, Borea PA, Somlo S, Del SL. Deficiency of polycystin-2 reduces Ca2+ channel activity and cell proliferation in ADPKD lymphoblastoid cells. FASEB J 2004;18:884–886. [PubMed: 15001556]

Arnould T, Kim E, Tsiokas L, Jochimsen F, Gruning W, Chang JD, Walz G. The polycystic kidney disease 1 gene product mediates protein kinase C alpha-dependent and c-Jun N-terminal kinase-dependent activation of the transcription factor AP-1. J Biol Chem 1998;273:6013–6018. [PubMed: 9497315]

Bhunia AK, Piontek K, Boletta A, Liu L, Qian F, Xu PN, Germino FJ, Germino GG. PKD1 induces p21 (waf1) and regulation of the cell cycle via direct activation of the JAK-STAT signaling pathway in a process requiring PKD2. Cell 2002;109:157–168. [PubMed: 12007403]

Boulter C, Mulroy S, Webb S, Fleming S, Brindle K, Sandford R. Cardiovascular, skeletal, and renal defects in mice with a targeted disruption of the Pkd1 gene. Proc Natl Acad Sci U S A 2001;98:12174–12179. [PubMed: 11593033]

Brault V, Moore R, Kutsch S, Ishibashi M, Rowitch DH, McMahon AP, Sommer L, Boussadia O, Kemler R. Inactivation of the beta-catenin gene by Wnt1-Cre-mediated deletion results in dramatic brain malformation and failure of craniofacial development. Development 2001;128:1253–1264. [PubMed: 11262227]

Brewer S, Feng W, Huang J, Sullivan S, Williams T. Wnt1-Cre-mediated deletion of AP-2alpha causes multiple neural crest-related defects. Dev Biol 2004;267:135–152. [PubMed: 14975722]

Dabovic B, Chen Y, Colarossi C, Obata H, Zambuto L, Perle MA, Rifkin DB. Bone abnormalities in latent TGF-[beta] binding protein (Ltbp)-3-null mice indicate a role for Ltbp-3 in modulating TGF-[beta] bioavailability. J Cell Biol 2002a;156:227–232. [PubMed: 11790802]

Dabovic B, Chen Y, Colarossi C, Zambuto L, Obata H, Rifkin DB. Bone defects in latent TGF-beta binding protein (Ltbp)-3 null mice; a role for Ltbp in TGF-beta presentation. J Endocrinol 2002b; 175:129–141. [PubMed: 12379497]

Day TF, Guo X, Garrett-Beal L, Yang Y. Wnt/beta-catenin signaling in mesenchymal progenitors controls osteoblast and chondrocyte differentiation during vertebrate skeletogenesis. Dev Cell 2005;8:739–750. [PubMed: 15866164]

Delmas P. Polycystins: polymodal receptor/ion-channel cellular sensors. Pflugers Arch 2005;451:264–276. [PubMed: 15889307]

Dudas M, Sridurongrit S, Nagy A, Okazaki K, Kaartinen V. Craniofacial defects in mice lacking BMP type I receptor Alk2 in neural crest cells. Mech Dev 2004;121:173–182. [PubMed: 15037318]

Eswarakumar VP, Monsonego-Ornan E, Pines M, Antonopoulou I, Morriss-Kay GM, Lonai P. The IIIc alternative of Fgfr2 is a positive regulator of bone formation. Development 2002;129:3783–3793. [PubMed: 12135917]

Fitzgerald JB, Jin M, Grodzinsky AJ. Shear and compression differentially regulate clusters of functionally related temporal transcription patterns in cartilage tissue. J Biol Chem 2006;281:24095–24103. [PubMed: 16782710]

Forman JR, Qamar S, Paci E, Sandford RN, Clarke J. The remarkable mechanical strength of polycystin-1 supports a direct role in mechanotransduction. J Mol Biol 2005;349:861–871. [PubMed: 15894330]

Grodzinsky AJ, Levenston ME, Jin M, Frank EH. Cartilage tissue remodeling in response to mechanical forces. Annu Rev Biomed Eng 2000;2:691–713. [PubMed: 11701528]

Guillaume R, D'Agati V, Daoust M, Trudel M. Murine Pkd1 is a developmentally regulated gene from morula to adulthood: role in tissue condensation and patterning. Dev Dyn 1999;214:337–348. [PubMed: 10213389]

Hou B, Fukai N, Olsen BR. Mechanical force-induced midpalatal suture remodeling in mice. Bone. 2007

Hughes J, Ward CJ, Peral B, Aspinwall R, Clark K, San Millan JL, Gamble V, Harris PC. The polycystic kidney disease 1 (PKD1) gene encodes a novel protein with multiple cell recognition domains. Nat Genet 1995;10:151–160. [PubMed: 7663510]

Kanno T, Takahashi T, Tsujisawa T, Ariyoshi W, Nishihara T. Mechanical stress-mediated Runx2 activation is dependent on Ras/ERK1/2 MAPK signaling in osteoblasts. J Cell Biochem. 2007

Kim K, Drummond I, Ibraghimov-Beskrovnaya O, Klinger K, Arnaout MA. Polycystin 1 is required for the structural integrity of blood vessels. Proc Natl Acad Sci U S A 2000;97:1731–1736. [PubMed: 10677526]

Kolpakova-Hart E, Jinnin M, Hou B, Fukai N, Olsen BR. Kinesin-2 controls development and patterning of the vertebrate skeleton by Hedgehog- and Gli3-dependent mechanisms. Dev Biol 2007;309:273–284. [PubMed: 17698054]

Li X, Luo Y, Starremans PG, McNamara CA, Pei Y, Zhou J. Polycystin-1 and polycystin-2 regulate the cell cycle through the helix-loop-helix inhibitor Id2. Nat Cell Biol 2005;7:1102–1112.

Low SH, Vasanth S, Larson CH, Mukherjee S, Sharma N, Kinter MT, Kane ME, Obara T, Weimbs T. Polycystin-1, STAT6, and P100 function in a pathway that transduces ciliary mechanosensation and is activated in polycystic kidney disease. Dev Cell 2006;10:57–69. [PubMed: 16399078]

Lu W, Peissel B, Babakhanlou H, Pavlova A, Geng L, Fan X, Larson C, Brent G, Zhou J. Perinatal lethality with kidney and pancreas defects in mice with a targetted Pkd1 mutation. Nat Genet 1997;17:179–181. [PubMed: 9326937]

Lu W, Shen X, Pavlova A, Lakkis M, Ward CJ, Pritchard L, Harris PC, Genest DR, Perez-Atayde AR, Zhou J. Comparison of Pkd1-targeted mutants reveals that loss of polycystin-1 causes cystogenesis and bone defects. Hum Mol Genet 2001;10:2385–2396. [PubMed: 11689485]

Malhas AN, Abuknesha RA, Price RG. Interaction of the leucine-rich repeats of polycystin-1 with extracellular matrix proteins: possible role in cell proliferation. J Am Soc Nephrol 2002;13:19–26. [PubMed: 11752017]

Movassaghi K, Altobelli DE, Zhou H. Frontonasal suture expansion in the rabbit using titanium screws. J Oral Maxillofac Surg 1995;53:1033–1042. [PubMed: 7643273]

Nagao S, Yamaguchi T, Kusaka M, Maser RL, Takahashi H, Cowley BD, Grantham JJ. Renal activation of extracellular signal-regulated kinase in rats with autosomal-dominant polycystic kidney disease. Kidney Int 2003;63:427–437. [PubMed: 12631108]

Nauli SM, Alenghat FJ, Luo Y, Williams E, Vassilev P, Li X, Elia AE, Lu W, Brown EM, Quinn SJ, Ingber DE, Zhou J. Polycystins 1 and 2 mediate mechanosensation in the primary cilium of kidney cells. Nat Genet 2003;33:129–137. [PubMed: 12514735]

Ogle RC, Tholpady SS, McGlynn KA, Ogle RA. Regulation of cranial suture morphogenesis. Cells Tissues Organs 2004;176:54–66. [PubMed: 14745235]

Opperman LA. Cranial sutures as intramembranous bone growth sites. Dev Dyn 2000;219:472–485. [PubMed: 11084647]

Parnell SC, Magenheimer BS, Maser RL, Zien CA, Frischauf AM, Calvet JP. Polycystin-1 activation of c-Jun N-terminal kinase and AP-1 is mediated by heterotrimeric G proteins. J Biol Chem 2002;277:19566–19572. [PubMed: 11912216]

Qian F, Wei W, Germino G, Oberhauser A. The nanomechanics of polycystin-1 extracellular region. J Biol Chem 2005;280:40723–40730. [PubMed: 16219758]

Rafferty KL, Herring SW. Craniofacial sutures: morphology, growth, and in vivo masticatory strains. J Morphol 1999;242:167–179. [PubMed: 10521876]

Riddle RC, Taylor AF, Genetos DC, Donahue HJ. MAP kinase and calcium signaling mediate fluid flow-induced human mesenchymal stem cell proliferation. Am J Physiol Cell Physiol 2006;290:C776–C784. [PubMed: 16267109]

Rodda SJ, McMahon AP. Distinct roles for Hedgehog and canonical Wnt signaling in specification, differentiation and maintenance of osteoblast progenitors. Development 2006;133:3231–3244. [PubMed: 16854976]

Saxen L, Sariola H. Early organogenesis of the kidney. Pediatr Nephrol 1987;1:385–392. [PubMed: 3153305]

Shibazaki S, Yu Z, Nishio S, Tian X, Thomson RB, Mitobe M, Louvi A, Velazquez H, Ishibe S, Cantley LG, Igarashi P, Somlo S. Cyst formation and activation of the extracellular regulated kinase pathway after kidney specific inactivation of Pkd1. Hum Mol Genet 2008;17:1505–1516. [PubMed: 18263604]

Shukla V, Coumoul X, Wang RH, Kim HS, Deng CX. RNA interference and inhibition of MEK-ERK signaling prevent abnormal skeletal phenotypes in a mouse model of craniosynostosis. Nat Genet 2007;39:1145–1150. [PubMed: 17694057]

Singh GD. Morphologic determinants in the etiology of class III malocclusions: a review. Clin Anat 1999;12:382–405. [PubMed: 10462736]

Soriano P. Generalized lacZ expression with the ROSA26 Cre reporter strain. Nat Genet 1999;21:70–71. [PubMed: 9916792]

Starremans PG, Li X, Finnerty PE, Guo L, Takakura A, Neilson EG, Zhou J. A mouse model for polycystic kidney disease through a somatic in-frame deletion in the 5′ end of Pkd1. Kidney Int 2008;73(12): 1394–405. [PubMed: 18385665]

The European Polycystic Kidney Disease Consortium. The polycystic kidney disease 1 gene encodes a 14 kb transcript and lies within a duplicated region on chromosome 16. The European Polycystic Kidney Disease Consortium. Cell 1994;78:725.

Wang X, Mao JJ. Chondrocyte proliferation of the cranial base cartilage upon in vivo mechanical stresses. J Dent Res 2002;81:701–705. [PubMed: 12351669]

Wealthall RJ, Herring SW. Endochondral ossification of the mouse nasal septum. Anat Rec A Discov Mol Cell Evol Biol 2006;288:1163–1172. [PubMed: 17031811]

Yin L, Du X, Li C, Xu X, Chen Z, Su N, Zhao L, Qi H, Li F, Xue J, Yang J, Jin M, Deng C, Chen L. A Pro253Arg mutation in fibroblast growth factor receptor 2 (Fgfr2) causes skeleton malformation mimicking human Apert syndrome by affecting both chondrogenesis and osteogenesis. Bone 2008;42:631–643. [PubMed: 18242159]

Yu K, Xu J, Liu Z, Sosic D, Shao J, Olson EN, Towler DA, Ornitz DM. Conditional inactivation of FGF receptor 2 reveals an essential role for FGF signaling in the regulation of osteoblast function and bone growth. Development 2003;130:3063–3074. [PubMed: 12756187]

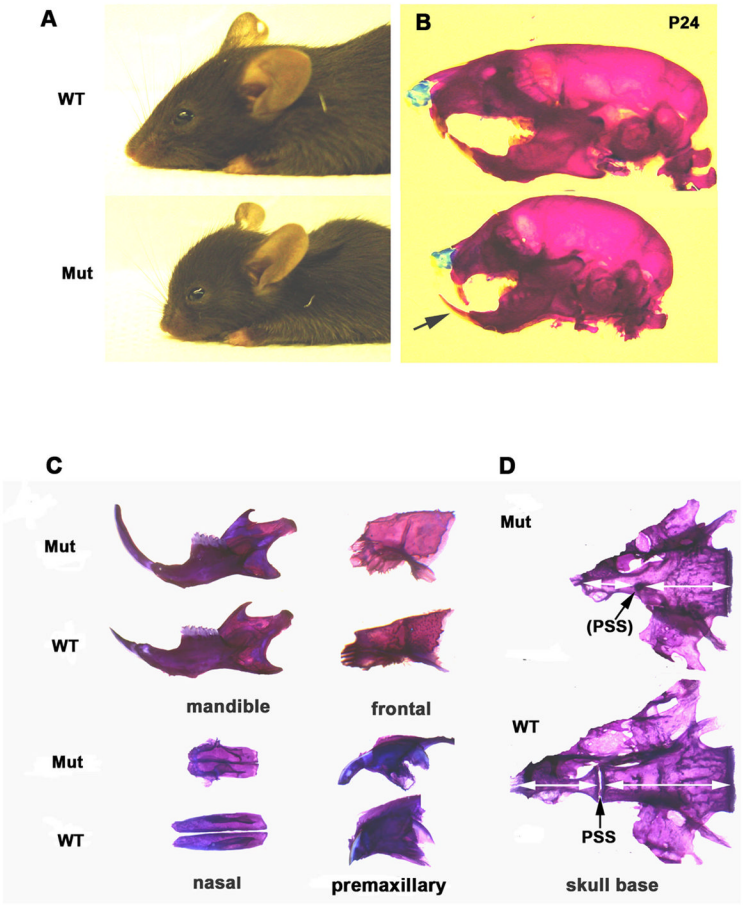

Fig. 1.

Neural crest-specific inactivation of *Pkd1* results in impaired postnatal growth of the rostral craniofacial skeleton and malocclusion. (A) Exterior morphology of wild type and conditional *Wnt1-Cre;Pkd1* mutants at weaning. (B) Alizarin red and Alcian blue staining of control and mutant skulls reveals a maxillary retraction and underbite (arrow) in *Pkd1*-deficient mice. (C) Comparative morphological studies of individual craniofacial bones from adult wild type and *Wnt1-Cre;Pkd1* mutant littermates stained with alizarin red reveal a mild longitudinal growth defect of the mutant mandible and frontal bone in contrast to the severely affected growth of the nasal and premaxillary bones. (D) Early postnatal obliteration of the presphenoid synchondrosis (arrow) in *Pkd1*-deficient mice results in the shortening of the sphenoid bones (double-headed arrows). Mut-*Wnt1-Cre;Pkd1/Pkd1*, WT- *Wnt1-Cre;Pkd1/+*.

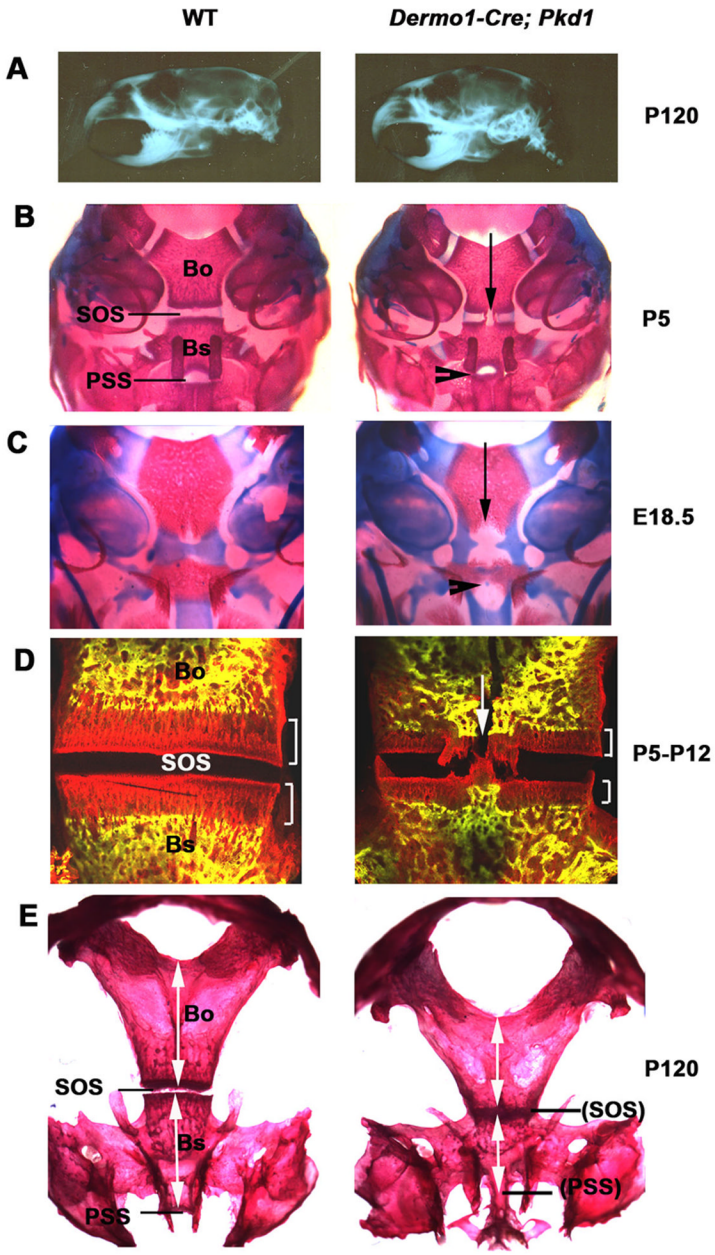

Fig. 2.

Reduced postnatal growth of the caudal neurocranium and the cranial base in *Dermo1-Cre;Pkd1* mice. (A) Representative radiograph of control and *Dermo1-Cre;Pkd1* skulls (lateral view) shows the dome-shaped neurocranium, a characteristic feature of the *Dermo1-Cre;Pkd1* mutant mice. (B) Ventral view of the cranium from 5-days old control and mutant mice. In the *Pkd1* knockout mice, an ossified contract is formed in the sphenooccipital synchondrosis (SOS) (arrow) and the presphenoid synchondrosis (PSS) is greatly reduced in size (arrowhead). (C) Alizarin red and Alcian blue staining of the E18.5 skulls demonstrates a wide open basicranial (arrow) and hypophyseal (arrowhead) fenestrae in the mutant cranial base. (D) Premature ossification of the sphenooccipital synchondrosis (arrow) impairs longitudinal growth of the cranial base. Double calcein/alizarin complexon in vivo labelling

shows decreased mineralization of the sphenoid and basisphenoid bones (brackets) between P5 and P12. (E) Dorsal view of the skull base from wild type and knockout adult mice reveals a reduced length of the basisphenoid and basioccipital bones (double-headed arrows) in *Dermo1-Cre;Pkd1* mice. The presphenoid and sphenooccipital synchondroses are closed in the mutant, whereas they remain patent in control mice. Bo-basioccipital bone, Bs-basisphenoid bone

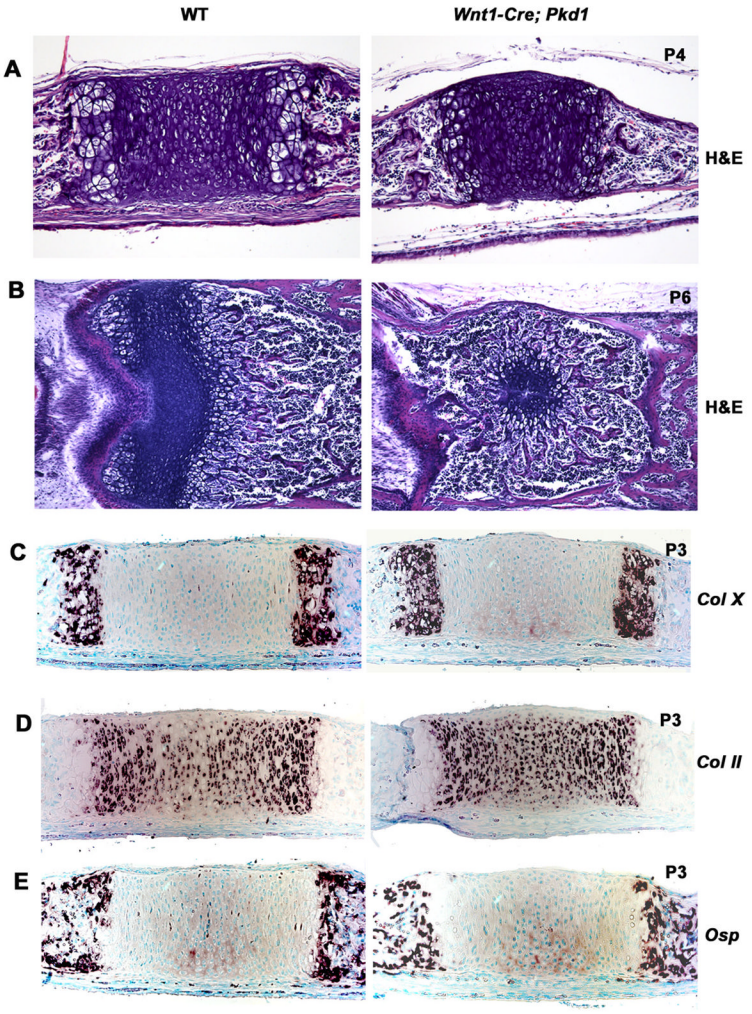

Fig. 3.

The distribution of the growth plate markers in the *Wnt1-Cre;Pkd1* presphenoidal synchondrosis is normal prior to its closure. (A) H&E staining of the parasagittal sections of control and mutant cranial base at P4 demonstrates a reduction in length of the *Pkd1*-deficient PSS prior to its closure. (B) H&E staining of the transverse sections of the control and mutant PSS at P6 shows premature closure for the mutant synchondrosis. (C-E) Expression pattern of the type X (C), type II (D) and *Osteopontin* in the P3 control and mutant PSS visualized by in situ hybridisation show no strong differences.

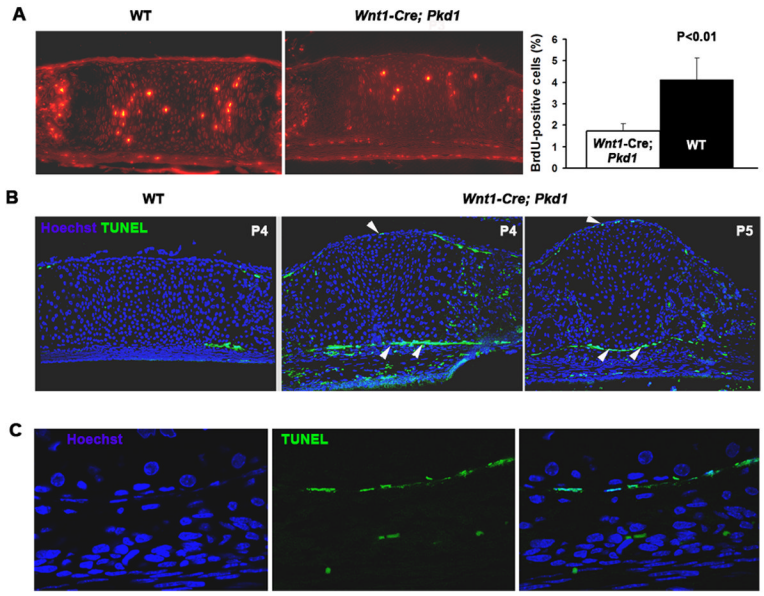

Fig. 4.

Pkd1-deficient presphenoid synchondrosis is characterized by a reduced proliferation of chondrocytes and increased apoptosis of the perichondrial cells. (A) Representative example of BrdU-specific staining of P3 presphenoid synchondrosis in control and *Wnt1-Cre;Pkd1* cranial base (left and middle panels). Proliferative rate of control (black bar) and *Pkd1*-deficient (white bar) PSS chondrocytes is shown as average percent of BrdU-positive cells relative to total cell population (n=5). All error bars are s.d., P<0.01, student t test (right panel). (B) TUNEL staining of the control and *Pkd1*-deficient presphenoid synchondrosis prior to its obliteration reveals cell death within the perichondrium of the mutant (arrowheads). (C) High magnification of the single layer of apoptotic cells in the perichondrium of the mutant PSS as its closure proceeds.

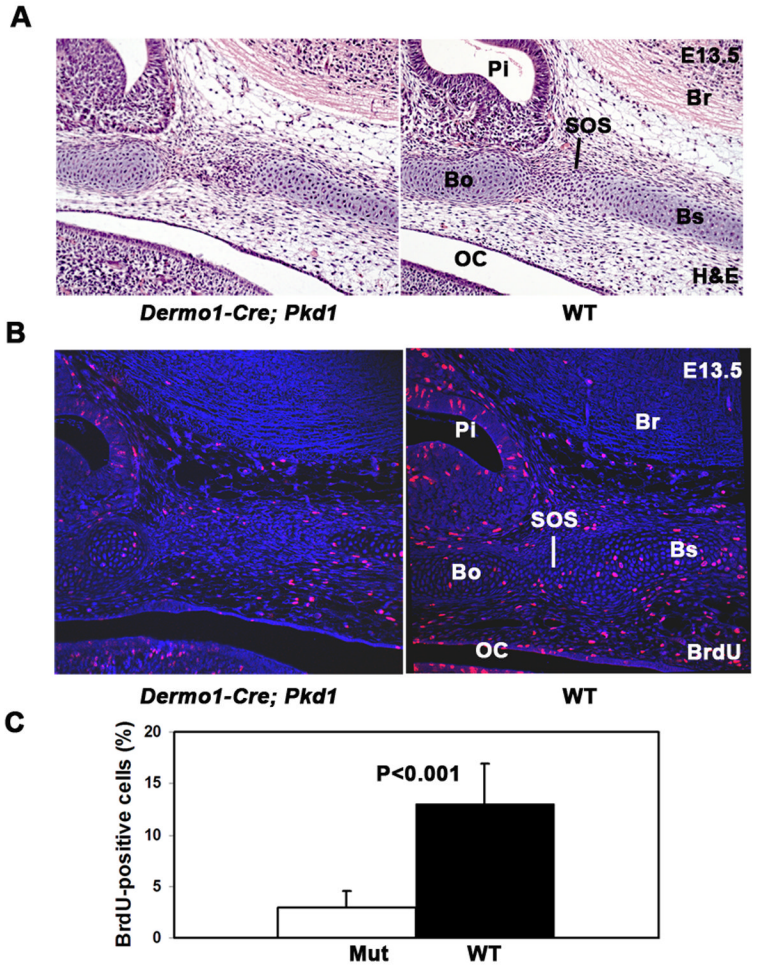

Fig. 5.

Proliferation of the mesenchymal osteichondroprogenitor cells and chondrocytes is greatly reduced in the cranial base of *Pkd1*-deficient embryos. (A-B) Parasagittal sections from E13.5 wild type and *Dermo1-Cre;Pkd1* cranial base stained with H&E (A) or BrdU-specific antibody and nuclear Hoechst dye. Reduced cellularity and decreased proliferative activity are evident in the cranial base of the *Pkd1* conditional knockout embryos. (C) Quantitative analysis of the proliferative rate of the mesenchymal and chondrocytes in the presumptive SOS region of the E13.5 control (black bar) and mutant (white bar) cranial base. (n=12). Error bars are s.d. Statistical significance was determined by student t test. Br-brain, OC-oral cavity, Pi-pituitary gland

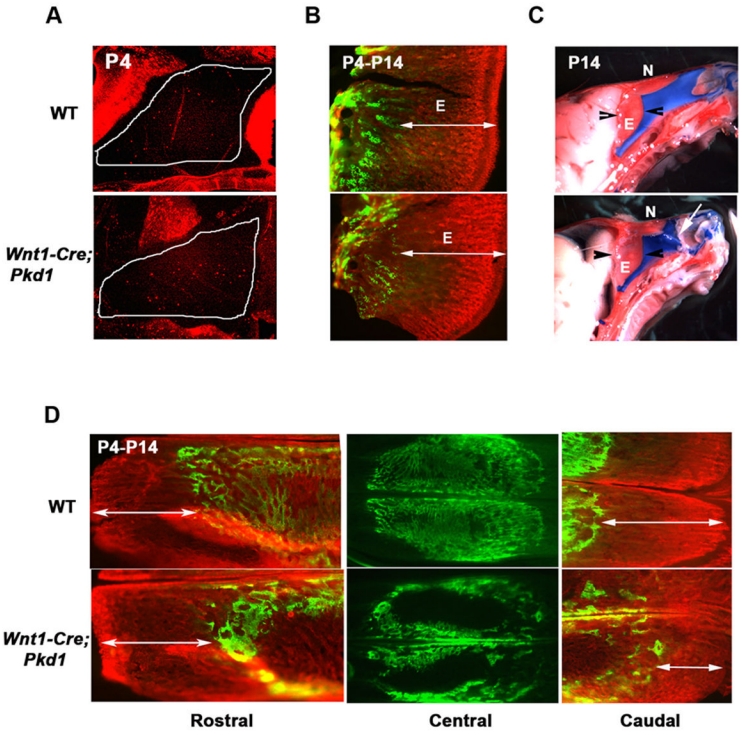

Fig. 6.

Wnt1-Cre;Pkd1 mice display normal proliferation and endochondral ossification of nasal septum, but reveal retarded growth of the caudal nasal bone. (A) Phosphorylated histone 3 labelling of the nasal cartilage (outlined) demonstrates a comparable level of interstitial chondrocytic proliferation in the mutant and control pups. (B) In vivo calcein and alizarin complexon double-labelling of bone tissue deposited on postnatal day 4 (green) and day 14 (red) demonstrates that the endochondral growth of the ethmoid bone is not affected by *Pkd1* inactivation, as its mineralization rate (double-headed arrows) is similar in the *Wnt1-Cre;Pkd1* and control littermates. (C) Impaired nasal bone growth in the *Pkd1* knockout mice results in lateral dislocation of the nasal cartilage (arrow). Arrowheads mark the limits of the ethmoid bone. (D) In vivo calcein/alizarin double-labelling of bone deposited on postnatal day 4 (green) and day 14 (red) shows normal growth of the mutant and wild type rostral nasal bone (left panels, double-headed arrows). In contrast, mineralization of the caudal nasal bone is markedly reduced in the *Pkd1*-deficient mice relative to control (right panels, double-headed arrows). Note a delay in postnatal intramembranous ossification evident in the nasal mutant bone relative to control (central panels). E-ethmoid bone, N-nasal bone

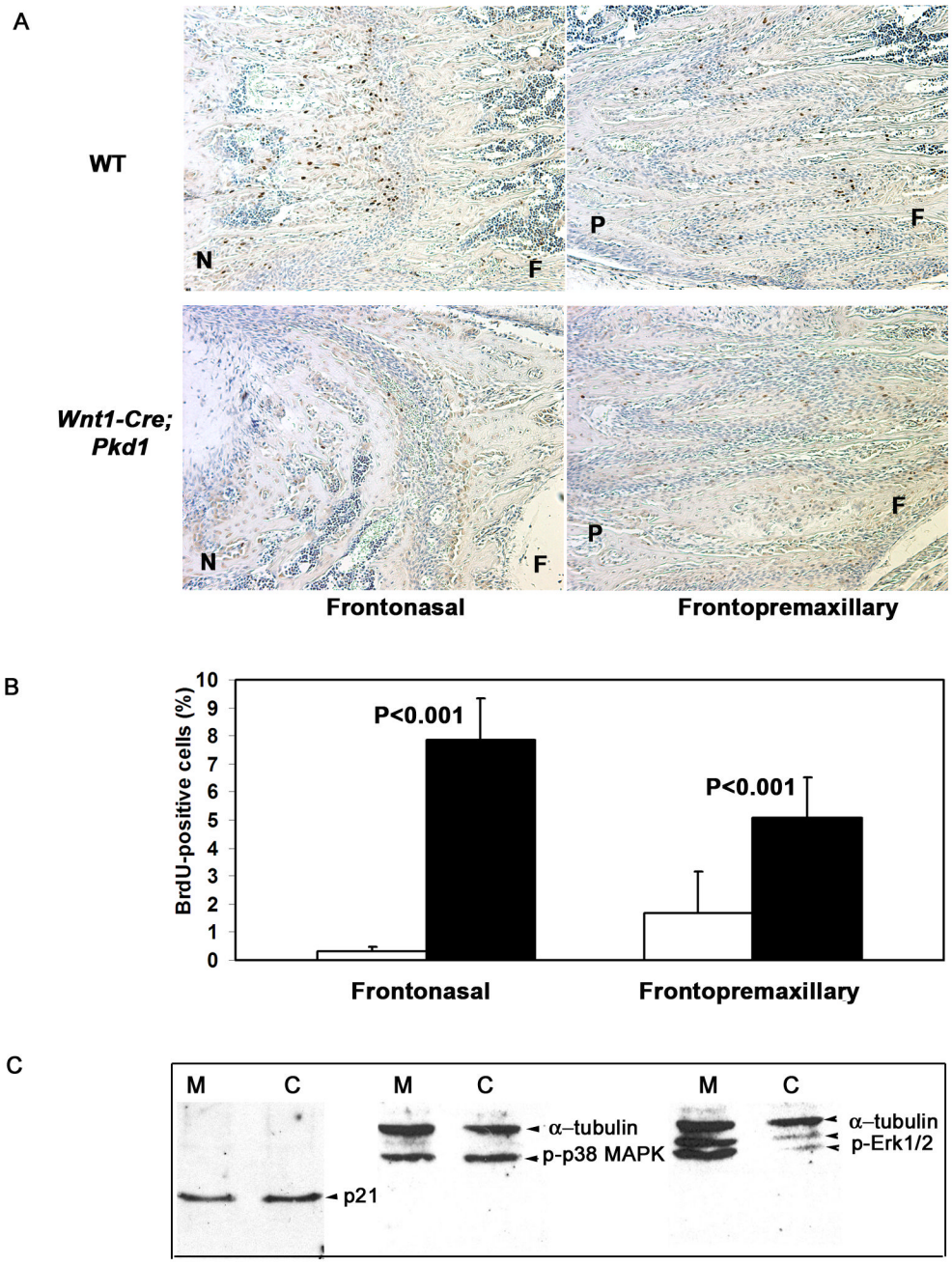

Fig. 7.

Pkd1-deficient facial bones display reduced proliferation of the sutural mesenchymal cells, yet Erk1 and Erk2 phosphorylation is up-regulated.

(A) BrdU-positive cells are observed at the osteogenic fronts in the frontonasal (top left panel) and the fronto-premaxillary (top right panel) wild type sutures. In *Pkd1* knockout mice, proliferation of the mesenchymal cells is undetectable in the frontonasal suture, whereas cell division in the fronto-premaxillary suture is significantly reduced. F-frontal, N-nasal, P-premaxillary bone.

(B) Proliferative rate of control (black bars) and *Pkd1*-deficient (white bars) sutural cells is shown as average percent of BrdU-positive cells relative to total cell population (n=10 for

frontonasal suture, n=12 for frontopremaxillary suture). All error bars are s.d., P<0.001, student t test.

(C) Expression levels of p21 and the phosphorylated form p38 MAPK are not affected in *Pkd1*-null sutures, whereas the Erk1/2 activity is elevated.

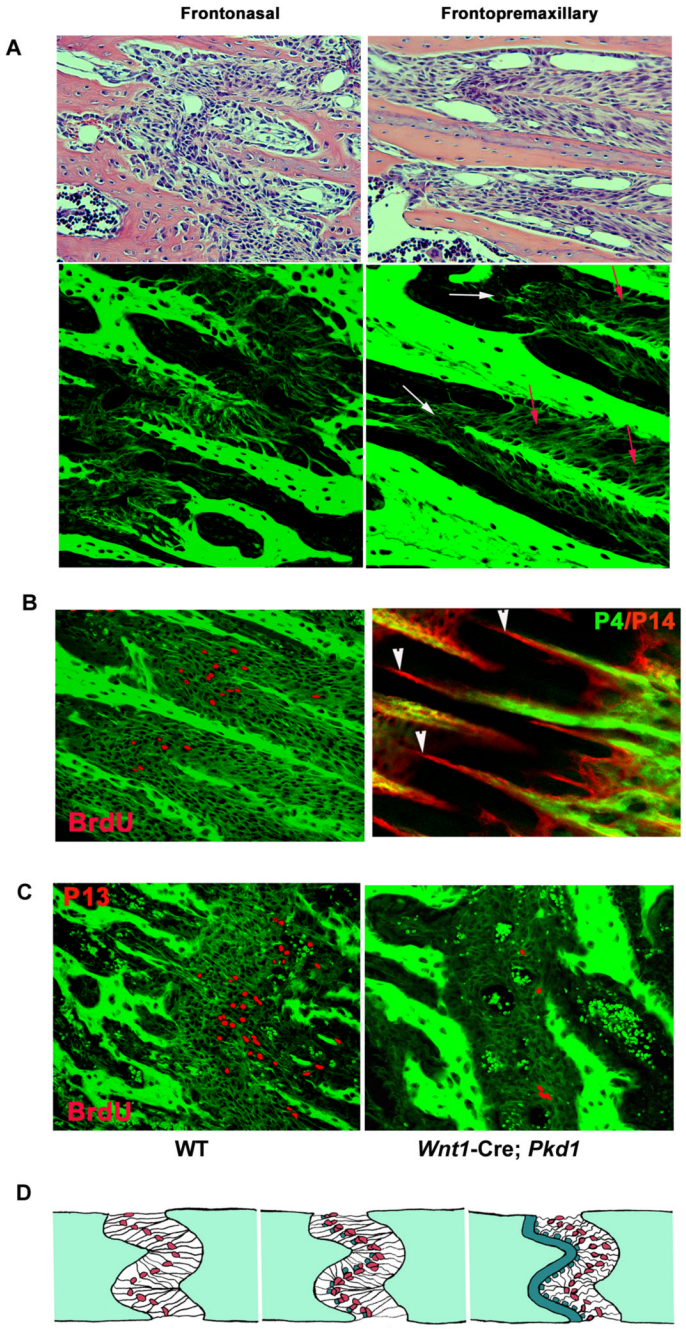

Fig. 8.

Collagen fibres organisation, mesenchymal cell proliferation and directional bone deposition in growing craniofacial sutures. (A) Upper panel: H&E staining of transverse sections through the frontonasal and frontopremaxillary sutures in growing mice (P22). Lower panel: confocal single scanning images of H&E stained transverse sections of the wild type frontonasal and fronto-premaxillary sutures (P22) visualises topology of collagen fibres and osteogenic fronts. The frontonasal suture displays a tension-specific arrangement of collagen fibre bundles, whereas the fronto-premaxillary suture appears largely compressed with obliquely oriented collagen fibres (red arrows). However, the suture areas around growing osteogenic fronts reveal presence of tensile forces in the suture (white arrows). (B) Left panel: BrdU staining of the

frontopremaxillary suture was performed using immunohistochemical labelling and BrdU-positive cells were artificially coloured in red. Right panel: in vivo calcein-alizarin double labelling of the fronto-premaxillary suture demonstrates that the sites of increased mesenchymal cell proliferation coincide with the sites of active bone deposition. (C) BrdU-positive cells visualized in the wild-type and *Pkd1*-defficient frontonasal sutures superimposed onto fluorescense images of the osteoid and collagen fibers in the suture. (D) Postnatal growth of the craniofacial skeleton in response to tensile forces. Left panel: in a suture of growing craniofacial skeleton, extracellular matrix fibres are stretched in response to tensile forces. Mesenchymal osteoprogenitor cells are found in close contact with collagen fibres where they are subjected to mechanical stress applied by growing nasal septum. Middle panel: mesenchymal cells in a suture respond to growth-induced tension by increased proliferation of pre-osteoblastic cells resulting in an increased number of differentiated osteoblasts. Right panel: enlarged population of osteoblasts relocate to osteogenic fronts of growing craniofacial bones and is responsible for the directional bone-specific extracellular matrix deposition and longitudinal bone growth.